Applied Energy 86 (2009) 355–363

Contents lists available at ScienceDirect

Applied Energy

journal homepage: www.elsevier.com/locate/apenergy

Design of a high frequency Inductively Coupled Power Transfer system for electric vehicle battery charge

Juan Luis Villa *, Jesús Sallán, Andrés Llombart, José Fco Sanz

CIRCE-University of Zaragoza, Electrical Engineering Department, C/María de Luna 3, 50018 Zaragoza, Spain

ARTICLE INFO

Article history:
Received 25 February 2008
Received in revised form 16 May 2008
Accepted 17 May 2008
Available online 27 June 2008

Keywords:
Inductive power transfer
Electric vehicles
Contact-less energy transfer
Compensation topologies

ABSTRACT

The development of a high autonomy purely electrical public mean of transportation is not currently viable because the required energy implies a very high battery weight. However, this weight would be significantly reduced if these batteries could be charged at the bus stops along the route, for instance using a contact-less power transfer system. An ICPT (Inductive Coupling Power Transfer) system with a large air gap has been developed and built for an electric vehicle battery charger. The practical sizing, the best compensation topology and the operational frequency have been studied in order to obtain maximum efficiency. The study has been focused on defining the prototype implementation process, validating the theoretical results and analyzing the influence of frequency deviation with respect to the resonant frequency and the effect of gap variation and misalignment in the behaviour of the system.

1. Introduction

In many applications, ICPT systems have several advantages over conventional energy transmission techniques using wires and connectors. For example, ICPT systems have been the preferred solution in hazardous applications due to the elimination of sparking and electrical shock risk [1]. The development of such systems is improving and the number of applications where they are suitable grows steadily: contact-less power supplies for professional tools [2], contact-less battery charging across large air gaps for electric vehicles [3], compact electronic devices [4], mobile phones [5] and public transport systems [6].

Generally, an ICPT is implemented using magnetic induction in specially constructed transformers. In such transformers, the energy is inductively transferred from the primary to the secondary through the air. It is quite common that ICPT systems have a relatively large separation between the primary and secondary winding (Fig. 1). Therefore, the characteristics of these transformers are very different from those of conventional transformers having good coupling between windings.

Due to a large winding separation, ICPT systems have relatively large leakage inductance and reduced magnetizing flux, which implies the need for greater magnetizing current.

All these features make the power factor to be low in both the primary and secondary sides reducing significantly the efficiency of the system. To improve the behaviour of ICPT systems several studies have been carried out in order to determine the best way of power factor compensation. In [7,8] different compensation schemes are proposed and their benefits are presented. In spite of these studies the design procedure is not clear. In [9] a design procedure is presented but there still remain many design decisions that depend on the actual case, which implies that the design procedure requires the development of four steps:

- Determining the minimum electrical requirements (voltage on both sides and power to be transferred to the load).
- Performing a first theoretical study.
- Simulating the approach.
- Testing experimentally the final approach.

The different studies consider a high distance between primary and secondary side something like 5 cm. We consider that for public transport this may be too short and, in addition, in such applications it is difficult to achieve constant gap and perfect winding alignment. So, to cover these questions, this paper studies the design of a 200 kW, 35 cm gap ICPT system and the design and test of a 5 kW laboratory-scale prototype with a 20 cm air gap. Simulating and testing this prototype, the influence of air gap variation and misalignment on the system behaviour is studied, focusing especially on the efficiency of the system.

There are other issues, not covered in this paper, that should be investigated, like the effect of the electromagnetic emissions associated with the ICPT system. These high frequency fields may affect the electronic equipment of the electric vehicle and some shielding could be required.

* Corresponding author. Tel.: +34 976762619; fax: +34 976762226.
E-mail address: jvilla@unizar.es (J.L. Villa).

0306-2619/$ - see front matter © 2008 Elsevier Ltd. All rights reserved.
doi:10.1016/j.apenergy.2008.05.009

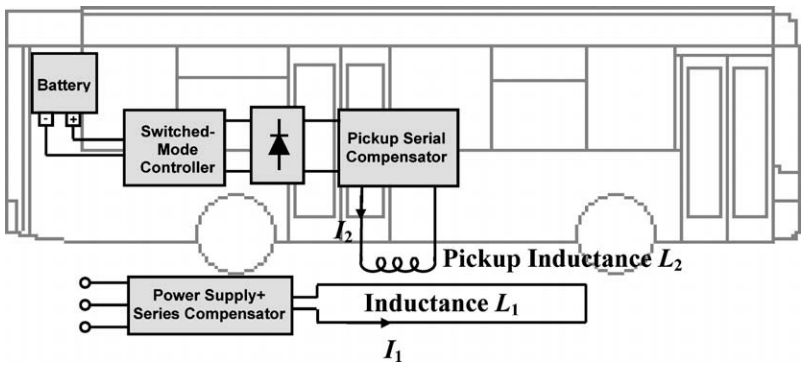

Fig. 1. Scheme of the ICPT battery charger.

2. ICPT theoretical model

The power transfer capability of an ICPT system depends directly on the coupling coefficient, k [1] which is given by

$$k = \frac{M}{\sqrt{L_1 L_2}} \tag{1}$$

where L_1 and L_2 are the self-inductance coefficients of the primary and secondary coils and M is the mutual inductance.

To improve the power transfer capability to the load, it is necessary to include capacitors in both sides. By working at the resonance frequency in the secondary selecting the appropriate capacitor C_2, the power transferred to the load is maximum. Selecting the capacitor in the primary side C_1 at this frequency, the total impedance of the system is purely resistive, so the current is in phase with the voltage and the source needs to deliver the minimum apparent power.

If Series–Series (SS) compensation is selected (i.e. both primary and secondary capacitors are connected in series with the respective coils), the primary capacitance is independent of both the magnetic coupling and the load [9]. The power transferred from the primary to the secondary is given by

$$P_2 = \frac{\omega_0^2 M^2}{R_L} I_1^2 \tag{2}$$

where ω_0 is the resonant frequency of the primary and secondary and is normally chosen [9]

$$\omega_0 = \frac{1}{\sqrt{L_1 C_1}} = \frac{1}{\sqrt{L_2 C_2}} \tag{3}$$

Thus, the capacitance values for C_1 and C_2 are:

$$C_1 = \frac{1}{\omega_0^2 L_1} \tag{4}$$

$$C_2 = \frac{1}{\omega_0^2 L_2} \tag{5}$$

To obtain the theoretical values for L_1, L_2 and M for the geometry shown in Fig. 2, the following expressions must be used:

L_1 is given by

$$L_1 = \frac{\mu_0}{\pi} N_1^2 \left[d \cdot \ln \frac{2Ld}{R_1\left(d + \sqrt{L^2 + d^2}\right)} \right] + \frac{\mu_0}{\pi} N_1^2 \left[L \cdot \ln \frac{2Ld}{R_1\left(L + \sqrt{L^2 + d^2}\right)} - 2\left(d + L - \sqrt{d^2 + L^2}\right) \right] + \frac{\mu_0}{4\pi} N_1^2 (L + d) \tag{6}$$

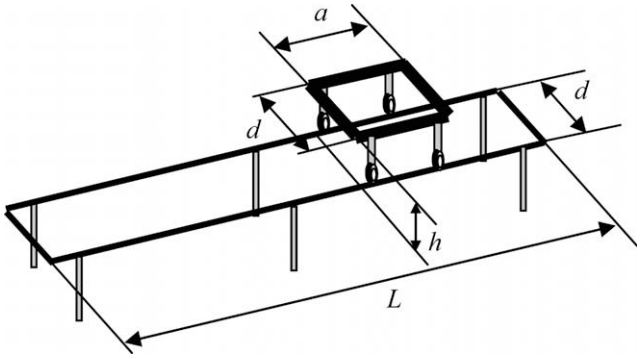

Fig. 2. Schematic of the implemented model showing design parameters.

and L_2 is given by

$$L_2 = \frac{\mu_0}{\pi} N_2^2 \left[d \cdot \ln \frac{2ad}{R_2\left(d + \sqrt{a^2 + d^2}\right)} \right] + \frac{\mu_0}{\pi} N_2^2 \left[a \cdot \ln \frac{2ad}{R_2\left(a + \sqrt{a^2 + d^2}\right)} - 2\left(d + a - \sqrt{d^2 + a^2}\right) \right] + \frac{\mu_0}{4\pi} N_2^2 (a + d) \tag{7}$$

where R_1 and R_2 are the equivalent radius of the windings.

$$R_1 = \sqrt{\frac{N_1 S_1}{\pi}} \tag{8}$$

$$R_2 = \sqrt{\frac{N_2 S_2}{\pi}} \tag{9}$$

If both coils have the same dimensions, the mutual inductance coefficient is given by

$$M = \frac{\mu_0}{\pi} N_1 N_2 \left[d \ln \frac{d + \left(\sqrt{h^2 + d^2}\right)\left(\sqrt{h^2 + a^2}\right)}{d + h\sqrt{h^2 + d^2 + a^2}} \right] + \frac{\mu_0}{\pi} N_1 N_2 \left[a \ln \frac{a + \left(\sqrt{h^2 + d^2}\right)\left(\sqrt{h^2 + a^2}\right)}{a + h\sqrt{h^2 + d^2 + a^2}} \right] + \frac{\mu_0}{\pi} N_1 N_2 \left[2\left(h - \sqrt{h^2 + d^2} - \sqrt{h^2 + a^2} + \sqrt{h^2 + d^2 + a^2}\right) \right] \tag{10}$$

Considering a case where the primary track is significantly longer than the secondary pick-up ($L \gg a$) the mutual inductance can be approximated by

$$M = \frac{\mu_0}{\pi} N_1 N_2 a \ln\left[\frac{\sqrt{h^2+d^2}}{h}\right] \tag{11}$$

The resistive values of the windings can be calculated using

$$R_1 = \frac{1}{57} N_1 \frac{2(L+d)}{S_1} \tag{12}$$

$$R_2 = \frac{1}{57} N_2 \frac{2(a+d)}{S_2} \tag{13}$$

Working at secondary resonance frequency, the efficiency of the system is given by

$$\eta = \frac{R_L}{R_L+R_2} \frac{1}{1+\frac{R_1(R_L+R_2)}{\omega_0^2 M^2}} \tag{14}$$

In order to achieve maximum efficiency

$$f_0 \gg \frac{\sqrt{R_1(R_L+R_2)}}{2\pi} \tag{15}$$

where f_0 is the resonant frequency of the system. Eq. (2) shows that the better the coupling between the two coils, the lower the design frequency. A frequency factor K_ω can be defined as follows:

$$f_0 = K_\omega \frac{\sqrt{R_1(R_L+R_2)}}{2\pi} \tag{16}$$

K_ω must be greater than unity and should be determined for each turn combination in order to achieve optimum efficiency. Once this frequency is determined, the rest of the parameters shown in Fig. 3 can be obtained using the expressions summarized in Table 1.

3. Prototype design

A study on urban bus energy requirements carried out at the University of Zaragoza [11] establishes that for a conventional bus with 150 kW rated power and a maximum consumption cycle of 109 s, with two acceleration intervals and recovering energy during regenerative braking, the consumed energy would be 7.9 MJ/cycle. The energy recovered during braking would be 750 kJ/cycle and thus, the energy to be transferred between two consecutive stops would be 7.15 MJ/cycle. The transfer period is set to 35 s, so the required power is 200 kW.

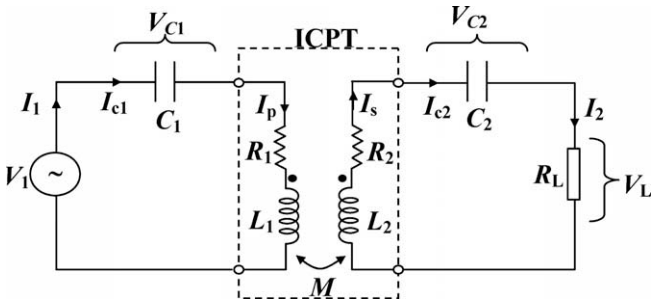

Fig. 3. Scheme of the implemented model and theoretical parameters.

Table 1
Expressions to determine the value of the electric parameters

Parameter	Equation
$\bar{Z}_T$	$\left(R_1 + j\left(L_1\omega - \frac{1}{C_1}\omega\right)\right) + \frac{\omega^2 M^2}{\left(R_2+R_L+j\left(L_2\omega-\frac{1}{C_2\omega}\right)\right)}$
$\bar{I}_1$	$\frac{\bar{V}_1}{\bar{Z}_T}$
$\bar{I}_{C1}$	$\bar{I}_P$
$\bar{V}_{C1}$	$\frac{\bar{I}_1}{jC_1\omega}$
$\bar{I}_2$	$M\frac{j\omega M\bar{I}_p}{\left(R_2+R_L+j\left(L_2\omega-\frac{1}{jC_2\omega}\right)\right)}$
$\bar{I}_{C2}$	$\bar{I}_s$
$\bar{V}_{C2}$	$\frac{\bar{I}_s}{jC_2\omega}$
P_L	$R_L I_2^2$
$\bar{V}_L$	$R_L\bar{I}_2$

In order to install the system in a bus, the dimensions shown in Fig. 2 would be h = 0.35 m, d = 1.2 m, L = 4 m and a = 1.2 m. The input voltage is V_1 = 540 V and the electric specifications in the load are P_L = 200 kW, V_L = 500 V.

Once the parameters related to the application of the ICPT system are chosen, the first issue is calculating the remaining parameters: number of turns and section for each winding, resonant frequency and compensation capacitances. To do these calculations, the different equations that define the ICPT system behaviour (shown in Section 2) have been implemented in a Matlab program.

This model calculates the resonant frequency, capacitors C_1 and C_2, voltages across the capacitors V_{C1}, V_{C2}, primary power P_1, power in the load P_2, primary and secondary currents I_1 and I_2, and efficiency.

The iterative process shown in Fig. 4 is carried out in order to find the parameters that optimize the efficiency while minimizing the voltage across the resonant capacitors.

This process starts with a single turn in both primary and secondary windings of predefined sections. Next, the self and mutual inductances are calculated using Eqs. (6), (7) and (10) and the frequency that makes possible the transfer of the required power is determined. After that, current densities are checked and sections are increased if required. This process continues until the maximum number of turns in each winding is considered.

The best configuration is the one giving the required power with the lowest copper quantity and an operating frequency below the specified maximum value.

The results for the 200 kW ICPT system are summarized in Table 2.

A 5 kW prototype has been built to test the behaviour of the system, especially when suffering distance variations and lateral misalignment.

The air gap value is set to 20 cm and the dimensions shown in Fig. 2 are h = 0.2 m, d = 1.2 m, L = 4 m and a = 1.2 m. The electric specifications in the load are P_L = 5 kW, V_L = 60 V. The maximum allowed current densities are $\delta_{1max} = \delta_{2max}$ = 4 A/mm^2. The power is fixed by the application and the voltage is adjusted to charge a battery set composed of four 12 V elements. Once power and voltage are set, the equivalent load resistance is R_2 = 0.7287 Ω, and the secondary current I_2 = 83.3 A.

For the prototype, the obtained number of coils was 7 in both sides and the sections of the windings were S_1 = 10 mm^2 and S_2 = 30 mm^2. The initial parameter values are given in Table 1a and the equivalent circuit is shown in Fig. 5.

In the aforementioned calculations it has not been considered that the working frequency is high, so the real resistance values will differ from the calculated ones. Table 3 shows the theoretical versus the adjusted and real values.

4. Practical implementation

In order to validate the theoretical results, the 5 kW prototype shown in Fig. 6 has been built.

First, when the two coils were mounted, R_1, R_2, L_1 and L_2 were measured at 15.6 kHz and the results can be seen in Table 4b.

The inductance values obtained from the Matlab model were very close to the real values of the implemented prototype, but the resistances were higher because the values in (12) and (13)

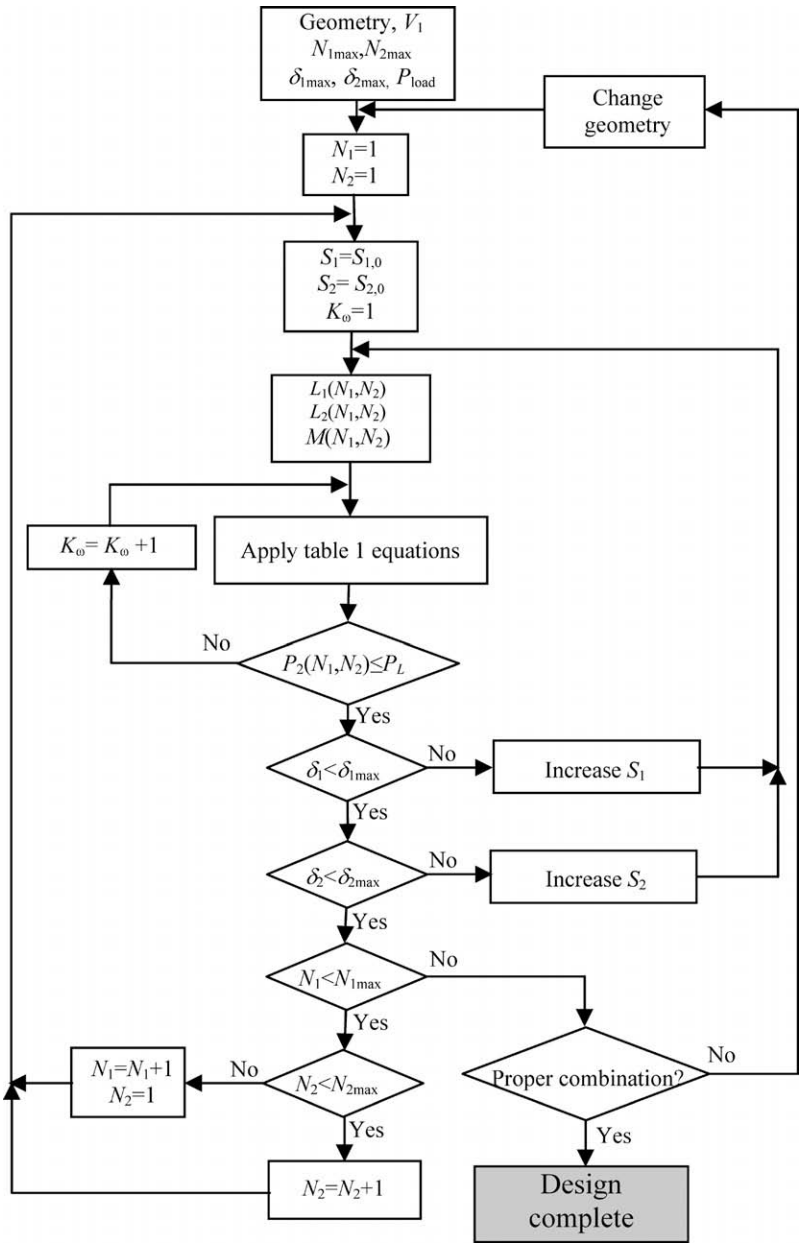

Fig. 4. Diagram of the iterative design process.

were calculated without taking into account the influence of the high frequency.

With these new values, the parameters of the Matlab model were recalculated and the results are shown in Table 3b.

The next step in the construction of the prototype was finding the capacitors. It was very difficult to get exactly the required capacitance, so the values were approximated. C_1 consisted of four 0.22 μF, 1000 V capacitors; C_2 consisted of fifteen 0.47 μF, 1000 V capacitors (Fig. 7).

With these definitive capacitors, the resonant frequency was 14.9 kHz and the results obtained with the Matlab model are given in Table 3c.

5. Response to gap variation and misalignment

In electric vehicle charge applications, there are two important aspects related to the distance between coils: the behaviour of the system when the gap is modified with respect to the design value, due to the variations in vehicle load (Fig. 8), and the stability of the system in the absence of secondary winding.

Fig. 9 shows that as the distance between coils is reduced, the transferred power is lower than the design value, showing a stable behaviour. This fact is due to the increase in the total impedance of the system, which causes a reduction in the consumed current I_1.

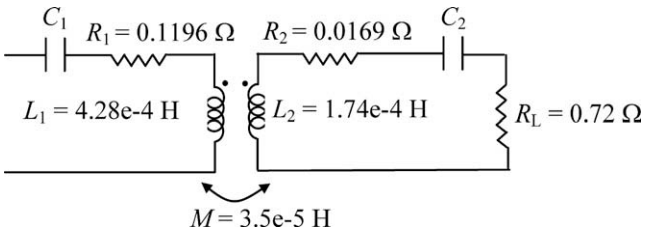

Fig. 5. Scheme of the implemented model and theoretical parameters.

Table 2
Parameters of the 200 kW CPT system

Parameter	Value
N_1	6
N_2	4
S_1 (mm^2)	94
S_2 (mm^2)	100
Copper (kg)	34.6
f_0 (kHz)	18
η (%)	97
P_2 (kW)	200
V_2 (V)	500
V_{C1} (V)	4590
V_{C2} (V)	2296
I_1 (A)	370
I_2 (A)	400
l_1 (mH)	0.109911
l_2 (mH)	0,05009
M (mH)	0.01188
k	0.16
C_1 (μF)	0.7121
C_2 (μF)	1.5329

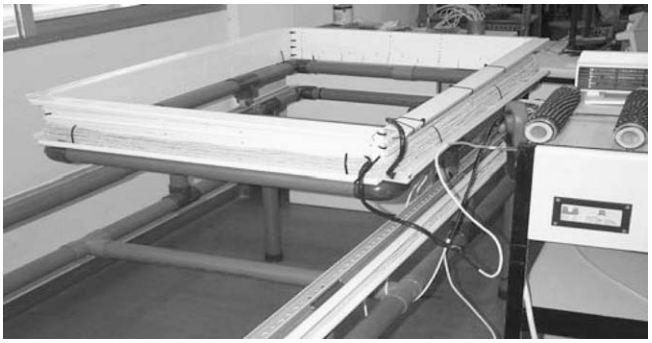

Fig. 6. Implementation of the proposed system with the long primary track and the pick-up.

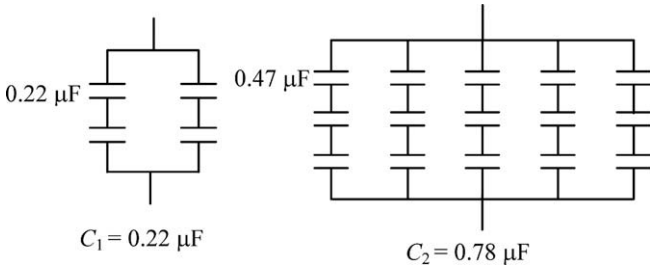

Fig. 7. Schemes of the capacitor sets.

When distance between coils is increased, power rises and in the limit, if the primary winding is fed in the absence of secondary winding, absorbed power is very high, which makes necessary

Table 3
Theoretical, adjusted and real values

Parameter	(a) Theoretical	(b) Adjusted	(c) Real
f_0	l.594le+004 Hz	15.6 kHz	14.9 kHz
k	0.1288	0.137	0.137
C_1	2.3257e−7 F	2.325e−7 F	2.2e−7
C_2	5.7222e−7 F	7,224e−7 F	7.8e−7
I_1	17.92A	18.73 A	19,88 A
I_1	83 A	83.35 A	82.08 A
V_{C1}	755 V	823.6 V	963.2 V
V_{C2}	1443 V	II77 V	1124 V
V_2	60.2 V	60.2 V	59.6
P_1	5150 W	5325 W	5445
P_2	4981 W	5002 W	4891
η	96.7%	93.9%	89.8%

Table 4
Theoretical values of Matlab model versus real values

	(a) Theoretical	(b) Practical
R_1	0.12 Ω	0.26 Ω
R_2	0.017 Ω	0.042 Ω
L_1	4.28e−4 H	4.48e−4 H
L_2	1.74e−4 H	1.44e−4 H

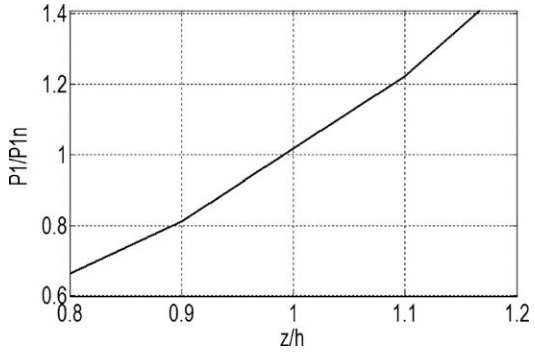

Fig. 9. P_1P_{1n} with a +20% gap variation (simulated).

the implementation of a control that detects the presence of the secondary pick-up.

Another important analysis is studying the variation in power transfer capability when a misalignment between coils occurs. Due to the fact that the primary winding is longer than the secondary winding, only misalignment in the *x*-axis is considered (Fig. 10).

Fig. 11 shows that when misalignment occurs, if frequency is kept constant, the absorbed power and the power transferred to the load increase significantly. However, a slight increase in the operating frequency (Fig. 12) keeps transferred power constant in its rated value, although this causes an increase in primary current because the system goes further out of resonance.

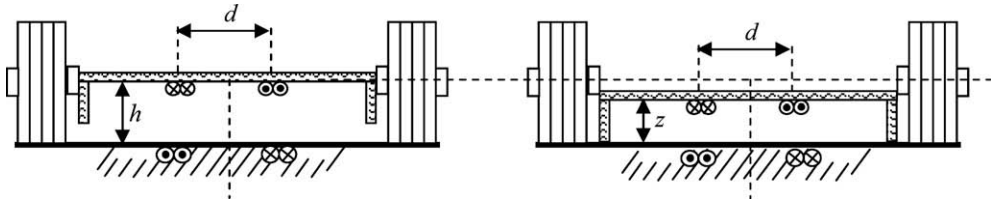

Fig. 8. Gap reduction due to load increase.

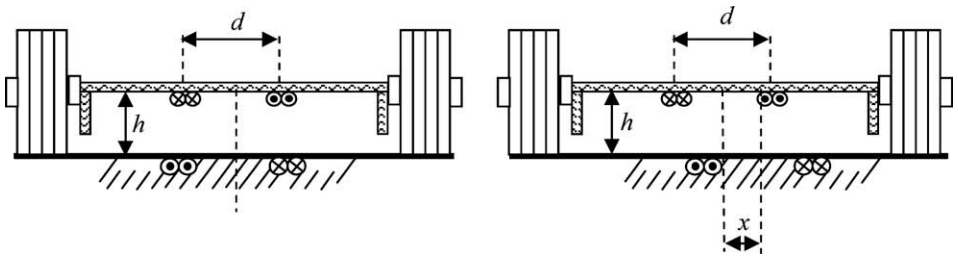

Fig. 10. Misalignment in the *x*-axis.

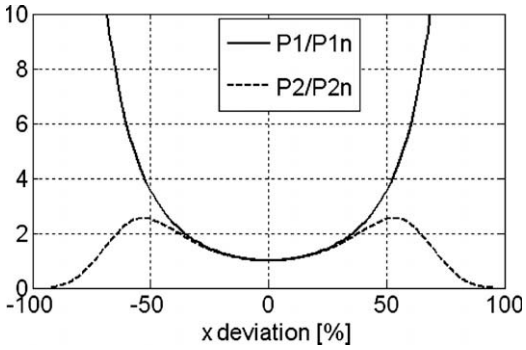

Fig. 11. P_1/P_{1n} and P_l/P_{2n} versus *x* misalignment (simulated).

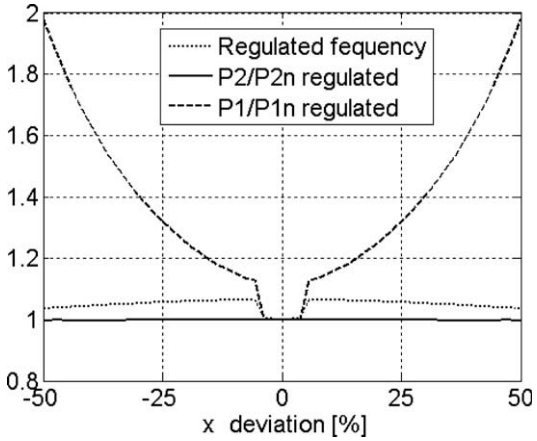

Fig. 12. Absorbed and transferred power with frequency regulation and required frequency variation.

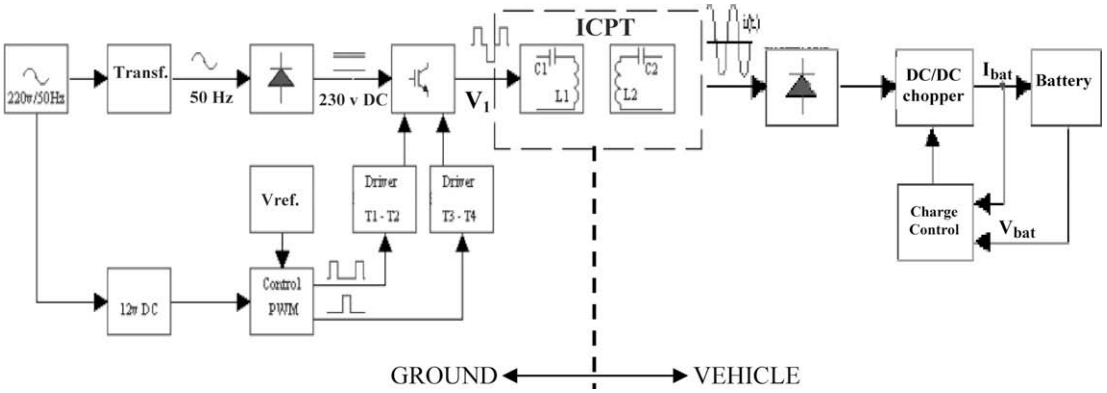

Fig. 13. Block diagram of the PWM control for the proposed system.

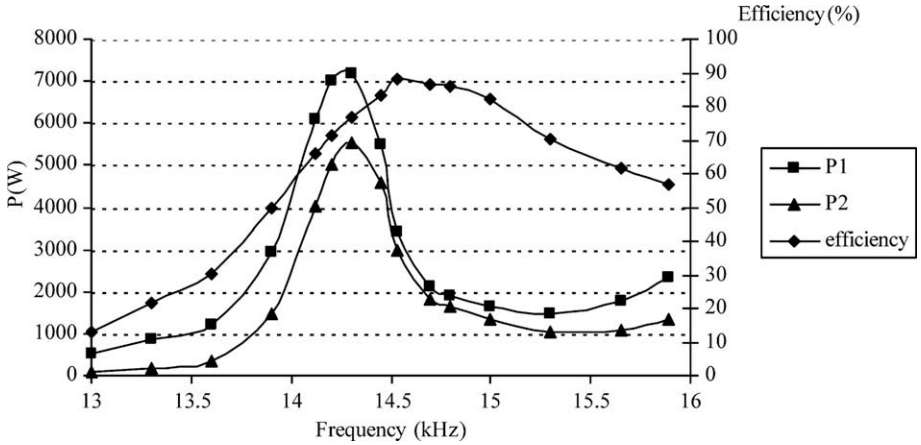

Fig. 14. Frequency variation of P_1, P_2 and efficiency.

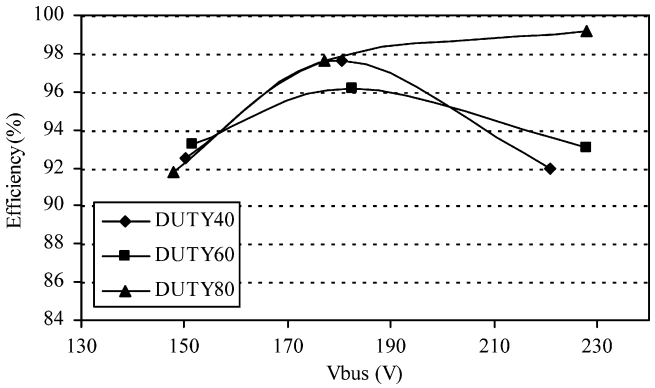

Fig. 15. Variation of the efficiency at resonant frequency for different DC voltages.

6. Experimental results

In order to validate the results obtained from the simulations, the primary of the ICPT system, described in the previous section, was fed with a square wave voltage provided by a full bridge inverter with PWM (Pulse Width Modulation) control [4], whose output voltage V_1 is controlled by the Duty Cycle (DC). The schematic of the whole system is shown in Fig. 13.

A PWM control is needed to avoid the transitory of the current. When the voltage is applied directly from the source, the current has a transient state of about 3 ms and the peak primary current is about 2.5 times the steady state peak value.

The first test was to check the frequency of optimum efficiency in the implemented prototype, in order to validate the model, and it was determined at $f = 14.55$ kHz, as shown in Fig. 14. This frequency is very close to the calculated theoretical resonant frequency, so the mathematical model is validated to design the ICPT. However, the real efficiency was a little lower than expected, 88.4% instead of 89.8%.

If frequency is lower than the resonant frequency, the power rises and the efficiency falls. However, if frequency is higher, both the power and the efficiency fall, so it is necessary to control the frequency of the primary to work always at maximum efficiency point [9,10].

A second test was carried out to observe the influence of the DC on the efficiency of the system at the resonant frequency, in order to check the effect when the ICPT is fed with a non-sinusoidal voltage waveform, as shown in Fig. 15. It was verified that the efficiency is dependent on the DC, because the current is less sinusoidal with low DC.

To show the influence of the distance between coils on the behaviour of the system, it can be seen in Figs. 16 and 17 how efficiency falls when distance increases. This result is interesting

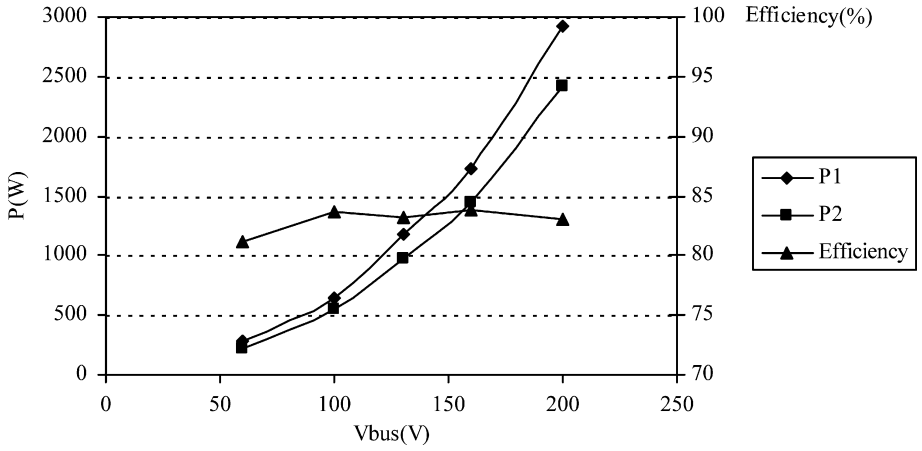

Fig. 16. P_1, P_2 and efficiency at 0.2 m and DC = 60%.

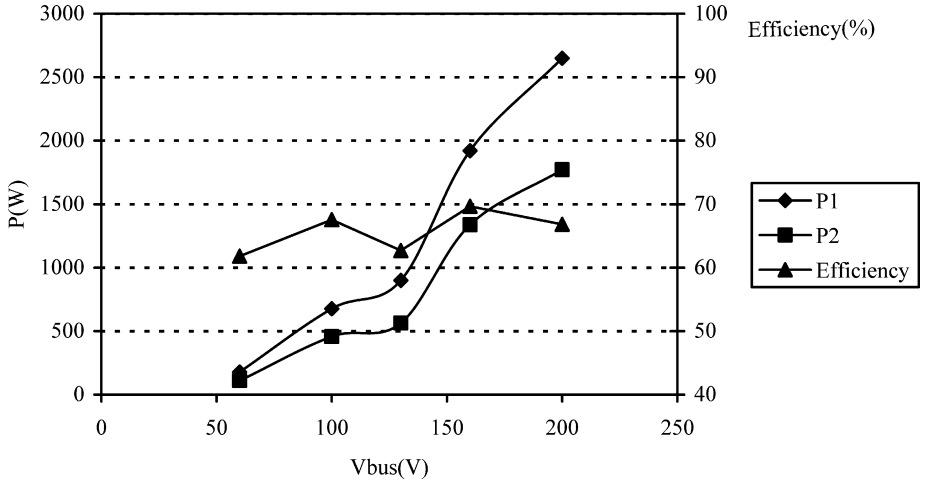

Fig. 17. P_1, P_2 and efficiency at 0.33 m and DC = 60%.

in order to control the power transfer capability to an electric vehicle when the air gap can vary depending on the weight of the vehicle.

As the distance between coils increases it is necessary to operate at higher frequencies to maintain the power transfer capability. Once more, a frequency control is required.

Fig. 18 shows experimental results that confirm the simulations. When distance between coils is reduced, the transferred power is lower than the design value, whereas if distance between coils grows, transferred power falls and the absorbed power increases.

To limit the change in transferred power when the air gap varies it is necessary to implement a frequency control. If the distance decreases, frequency has to be reduced whereas if the gap increases frequency must rise.

When distance is reduced a 20%, if frequency is not regulated the absorbed power decreases to 80% (Fig. 18), while decreasing the operating frequency the absorbed power only falls to 90% (Fig. 19) with a transferred power equal to 95%. If distance increases in the same percentage, unregulated absorbed power shows a 30% increase while adjusting the operating frequency the increase is only 13%, with a transferred power only 8% above its rated value.

Finally, tests were carried out to confirm the effect of misalignment in both the absorbed and the transferred power. Fig. 20 shows that the absorbed power increases and the transferred power initially increases slightly but for higher deviations

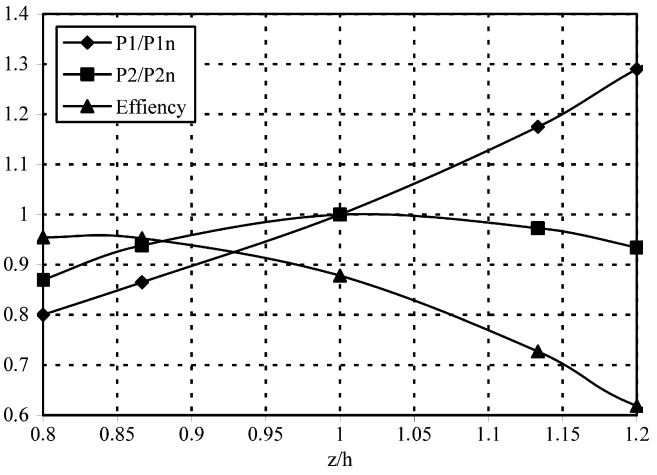

Fig. 18. P_1, P_2 and efficiency with a ±20% gap variation (experimental).

decreases, while efficiency is always below its rated value. However it is worth noticing that for misalignments up to $x = \pm 0.3$ p.u. the transferred power stays close to its rated value (having a primary power a 25% above its rated value). From this point on, the transferred power drops significantly while input power keeps rising. If both absorbed and transferred power are to be kept below their rated values, the working frequency of the system must be controlled.

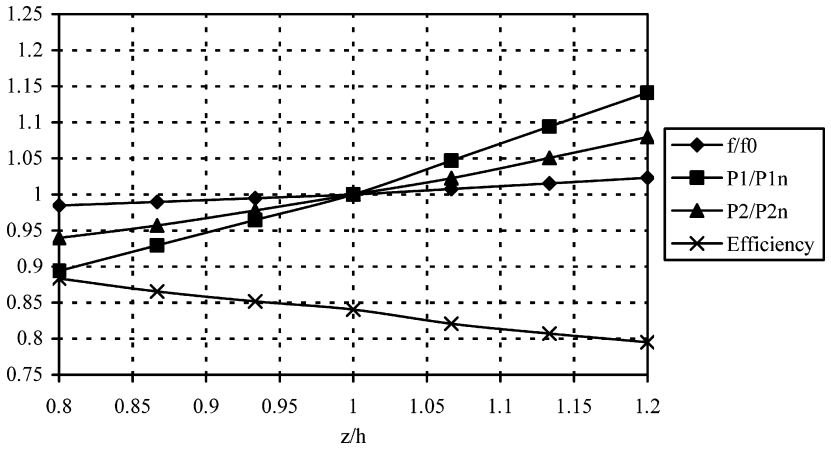

Fig. 19. P_1/P_{1n}, P_2/P_{2n} and efficiency with a ±20% gap variation with frequency regulation (experimental).

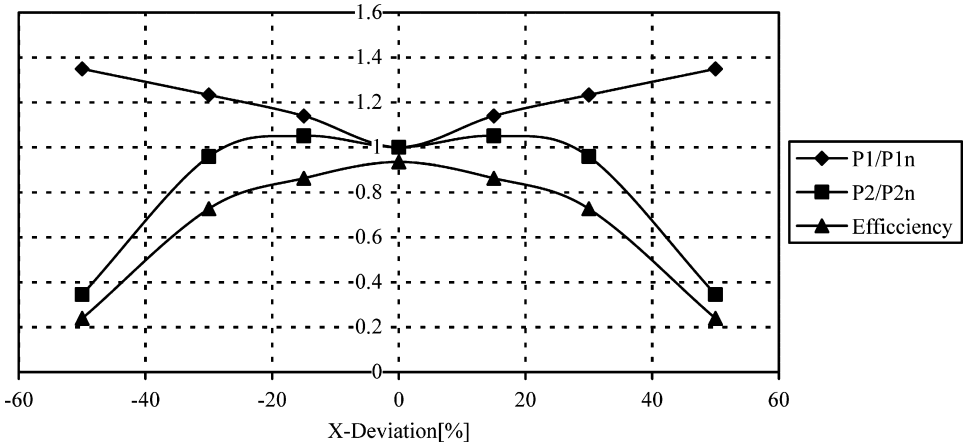

Fig. 20. P_1, P_2 and efficiency versus misalignment in x direction.

7. Conclusions

ICPT theory is well known, but in practice it is difficult to determine the parameters of the coils and the resonant frequency. Moreover, this frequency depends strongly on parameters such as the distance between coils, the load, and the shape of the current, so a good control is required in order to maintain the stability of the system.

This paper presents a procedure to determine the optimal configuration of a SS compensated ICPT system, which has been validated by the experimental results obtained in a 5 kW prototype.

Simulations and test have shown that efficiency and power transfer capability vary significantly if the air gap or the position of the pick-up can not be properly adjusted. However, if the frequency of the system is controlled, these parameters can be kept near their rated values even for gap variations up to 20% and misalignments up to 30%.

References

[1] Pedder DAG, Brown AD, Skinner JA. A contact-less electrical energy transmission system. IEEE Trans Ind Electron 1999;46(1):23–30.
[2] Bieler T, Perrotter M, Nguyen V, Perriard Y. Contact-less power and information transmission. In: Ind Applicat Conf 36 IAS annual meeting, vol. 1; 2001. p. 83–8.
[3] Laouner R, Brunello M, Ferrieux JP, Normand O, Buchheit N. A multi-resonant converter for noncontact charging with electromagnetic coupling. In: Proceedings IECON'97, vol. 2; 1997. p. 792–7.
[4] Abe H, Sakamoto H, Harada K. A noncontact charger using a resonant converter with parallel capacitor of the secondary coil. IEEE Trans Ind Applicat 2000;36(2):444–51.
[5] Jang Y, Jovanovic M. A contact-less electrical energy transmission system for portable–telephone battery chargers. Telecommun Energy Conf 2000: 726–32.
[6] Covic GA, Elliot G, Stielay OH, Green RM, Boys JT. The design of a contact-less energy transfer system for a people mover system. Int. Conf. Power System Technol. 2000;1:79–84.
[7] Wang CS, Covic GA, Stielau OH. Power transfer capability and bifurcation phenomena ofloosely coupled inductive power transfer system. IEEE Trans Ind Electron 2004;51(1):148–57.
[8] Wang CS, Covic GA, Stielau OH. Investigating an LCLload resonant inverter for inductive power transfer applications. IEEE Trans Ind Electron 2004;19(4): 995–1001.
[9] Wang CS, Stielau OH, Covic GA. Design consideration for a contactless electric vehicle battery charger. IEEE Trans Ind Electron 2005;52(5): 1308–13.
[10] Hu AP, Hussman S. Improved power flow control for contact-less moving sensor applications. IEEE Power Electron Lett 2004;2(4):135–8.
[11] Ubide-Querol D. Análisis de las Prestaciones de Autobuses Urbanos no Contaminantes. Ph.D. Thesis. University of Zaragoza (Spain); 2001.